



# Transverse Kinematics of Ion Stored in an Electrostatic Ion Beam Trap

Dina Attia, Daniel Strasser, Oded Heber, Michael Rappaport, Daniel Zajfman

## ► To cite this version:

Dina Attia, Daniel Strasser, Oded Heber, Michael Rappaport, Daniel Zajfman. Transverse Kinematics of Ion Stored in an Electrostatic Ion Beam Trap. 2005. hal-00004463

**HAL Id: hal-00004463**

**<https://hal.science/hal-00004463>**

Preprint submitted on 14 Mar 2005

**HAL** is a multi-disciplinary open access archive for the deposit and dissemination of scientific research documents, whether they are published or not. The documents may come from teaching and research institutions in France or abroad, or from public or private research centers.

L'archive ouverte pluridisciplinaire **HAL**, est destinée au dépôt et à la diffusion de documents scientifiques de niveau recherche, publiés ou non, émanant des établissements d'enseignement et de recherche français ou étrangers, des laboratoires publics ou privés.

# Transverse Kinematics of Ions Stored in an Electrostatic Ion Beam Trap

D. Attia <sup>a,b</sup> D. Strasser <sup>a</sup> O. Heber <sup>a</sup> M. L. Rappaport <sup>c</sup>  
D. Zajfman <sup>a</sup>

<sup>a</sup>*Department of Particle Physics, Weizmann Institute of Science, Rehovot 76100, Israel*

<sup>b</sup>*Laboratoire Kastler Brossel, École Normale Supérieure et Université Pierre et Marie Curie, Boite 74, 4 Place Jussieu, F-75252 Paris CEDEX 05, France*

<sup>c</sup>*Physics Services, Weizmann Institute of Science, Rehovot 76100, Israel*

---

## Abstract

We present experimental results, as well as numerical simulations, for the transverse velocity distribution of ions stored in an electrostatic ion beam trap. The measurements indicate that the transverse velocity spread is about 1% of the longitudinal velocity, and that the ions fill the whole transverse stable phase space. We also demonstrate that ion losses from the trap due to multiple scattering with molecules from the residual gas is an important factor limiting the lifetime of the beam.

*Key words:* ion traps, multiple scattering, cooling

---

## 1 Introduction

The use and development of ion trapping techniques, which started about 50 years ago [1], have led to a broad range of discoveries and new experiments in physics and chemistry. In particular, one can cite high precision spectroscopy, mass measurements, particle dynamics, nuclear and atomic processes and the measurement of fundamental constants [2]. During the last few years, a new type of ion trap has been developed in which ion beams, instead of ion clouds, are trapped[3,4]. This new trap stores particles using only electrostatic fields and works on a principle similar to that of an optical resonator. The main advantages of the trap are the possibility to trap fast (keV) beams without need of deceleration, the well defined beam direction, easy access to the trapped beam by various probes, and simple requirements in terms of external beam injection. Different types of experiments have already been performed with

these traps, such as the measurement of metastable state lifetimes of atomic and molecular ions [5,6], the lifetimes of metastable negative ions [7,8], and electron impact detachment cross sections of negative clusters [9]. Cluster cooling has also been observed [10]. Interesting dynamics of the ion motion have been discovered, such as self-bunching (due to the so-called negative mass instability phenomenon) and the possibility of using simple phase space manipulation to reduce the velocity spread [11,12]. Electrostatic ion storage rings [13,14] have also been used during the last several years in a variety of experiments [15,16].

Although the motion of the ions in the trap can be readily simulated, no measurements of the transverse velocity distribution (TVD) of the stored beam have hitherto been performed. The TVD is needed to understand the trapping efficiency, as well as the beam loss processes, especially the ones related to multiple scattering. We describe here the method that we have developed to characterize the TVD of the stored ions. The results are compared to numerical trajectory simulations, which confirm that multiple scattering is the dominant loss process in these traps, and that the available area of the stable transverse phase space directly influences the lifetime of the trapped ion beam.

## 2 Experimental setup

### 2.1 Ion trap

Figure 1 shows a schematic view of the electrostatic ion trap and the detection system. Two different setups were used for creating the ions. For light ions, an electron impact ionization source was used and the ions were mass selected with two magnets. For heavier species, a matrix assisted laser desorption and ionization (MALDI) [17] source was used to create an ion bunch, which was mass selected using time of flight. In both cases, the ions were accelerated to an energy of 4.2 keV. Three different types of ions were used in this work:  $\text{Au}^+$  ( $m=197$ ) and singly charged angiotensin II ( $m=1046$ ) (both produced by the MALDI source), and  $\text{Ar}^+$  ( $m=40$ ) (produced by the electron impact source). After focusing and collimation, the beam is directed into the ion trap along its axis. A complete description of the ion trap is given in Ref. [4], and only the details relevant for the present experiment will be given here.

The trap is made of two identical cylindrically symmetric “electrostatic mirrors” that both trap the beam in the longitudinal direction and focus it in the lateral direction. Upon injection, the entrance set of electrodes (left side in Fig. 1) is grounded so that the ion bunch can reach the exit mirror (right hand side in Fig. 1), where they are reflected. Before the reflected bunch reaches

the entrance electrodes, the potentials of these electrodes are rapidly switched on ( $\sim 100$  ns rise time) to the same values as those of the exit electrodes. For proper choices of voltages, the ions bounce back and forth between the two mirrors, their lifetime being limited mainly by collisions with the residual gas molecules. The low pressure in the trap, of the order of  $5 \times 10^{-10}$  Torr when the electron impact source was used, and  $4 \times 10^{-11}$  Torr for the MALDI setup, is maintained by a cryopump.

Each electrostatic mirror comprises eight electrodes. The potentials of the electrodes labeled  $V_1$  to  $V_4$  and  $V_z$  in Fig. 1 are independently adjustable. The other electrodes are always grounded. Thus the 228 mm long central region of the trap between the two innermost electrodes is essentially field-free. The diameter of the central hole is 16 mm in the outer six electrodes and 26 mm in the two innermost electrodes. The distance between the outermost electrodes is 407 mm.

In order for the ions to be trapped, the electrode potentials have to satisfy certain conditions. It is well known that many principles of geometric optics can be applied to ion optics. In fact, our trap is based on an optical resonator made of two cylindrically symmetric mirrors [18]. For an optical resonator with identical mirrors and a Gaussian beam, the stability criterion (for a beam close to the symmetry axis) is related to the focusing properties of the mirrors:

$$L/4 \leq f \leq \infty, \quad (1)$$

where  $f$  is the focal length of each mirror and  $L$  is the distance between them. This condition is easy to fulfill with the above design. Another obvious requirement is that the maximum potential on the mirror axis,  $V_{max}$ , has to be high enough to reflect the ions, i.e.,  $qV_{max} > E_k$ , where  $q$  is the charge of the ions and  $E_k$  is their kinetic energy.

Some important aspects of the design should be emphasized. First, the trap is completely electrostatic, so there is no limit on the mass that can be trapped. Second, the trapping depends only on the ratio  $E_k/q$ , which means that ions of different mass that are accelerated through the same potential difference can be stored simultaneously. Third, the central part of the ion trap is (nearly) field-free, so the ions travel in straight lines in this region.

Various electrode voltage configurations are possible to achieve trapping. We define a particular configuration by the set of potentials  $\{V_1, V_2, V_3, V_4, V_z\}$ .  $V_z$  is connected to the central electrode of an Einzel lens that plays the major role in determining the focusing properties of the mirrors. In the present work, only symmetric configurations, i.e., where identical potentials are applied to the two mirrors, are considered. The potentials on the four outmost electrodes were set to  $\{V_1, V_2, V_3, V_4\} = \{6.5, 4.875, 3.25, 1.65\}$  kV, while the Einzel voltage

was varied between  $2700 < V_z < 3200$  V and  $4000 < V_z < 4300$  V. These two ranges correspond to the known values where the trap is stable, i.e., they satisfy the criterion Eq. 1, as has been shown in Ref. [18]. Additional details about trapping stability and the comparison to optical models can be found in the literature[18].

## 2.2 Detection system

One of the ion loss processes from the trap is charge exchange, which leads to neutralization of the stored particles. These neutral particles pass freely through the mirrors and can be detected by a microchannel plate (MCP) detector located downstream of the trap (see Fig. 1). The detector is coupled to a phosphor screen so that the spatial distribution of the neutral particles exiting the trap can be imaged. The location and size of the MCP was different for the two different ion source setups used in this work: The MCP was 25 mm in diameter, and located at a distance of 80.3 cm from the center of the trap for the MALDI setup, while for the electron impact ionization source the MCP was 40 mm in diameter, and located at a distance of 90.3 cm from the center of the trap. The imaging is performed by a charge-coupled device (CCD) camera located outside the vacuum that is connected to a frame grabber which digitizes the picture in real time. The first image is taken in coincidence with the raising of the potentials on the entrance mirror, and subsequent images are digitized at a rate of 25 Hz for the whole trapping time ( $\sim 1$  s). The positions of impact ( $(x, y)$  on the front surface of the MCP) are determined for all hits producing an amount of light (as measured by the CCD camera) above a preprogrammed threshold. Images of about 50 to 150 injections are averaged to produce statistically significant results. The radial coordinate  $r$  is calculated as

$$r = \sqrt{(x - x_0)^2 + (y - y_0)^2} \quad (2)$$

where  $(x_0, y_0)$  is the point where the trap axis crosses the detector plane. This point is determined at a later stage by finding the center of the measured radial distribution.

## 2.3 Data analysis

In order to study the TVD inside the trap, we analyze the radial distribution of the neutral particles hitting the MCP detector. Fig. 1 shows the relationship between the ion position and velocity inside the trap at the instant of its

neutralization, and the point of impact of the neutralized particle on the detector,  $r$ . The ion's position at the neutralization point is given by its distance  $R$  from the optical axis of the trap and distance from the MCP,  $s$ . The ion's velocity at the same point is defined in terms of its longitudinal and transversal velocities  $v_{\parallel}$  and  $v_{\perp}$ , respectively (see Fig. 1). If we assume that the angular scattering taking place during the charge exchange is small compared to the angular dispersion of the beam (a very good approximation for the heavy ions created in the MALDI source)[19], then the position of impact on the MCP can be calculated from

$$r = R + \frac{sv_{\perp}}{v_{\parallel}}. \quad (3)$$

If we also use the fact that  $R \ll r$ , then we obtain for the transverse velocity

$$v_{\perp} = \frac{rv_{\parallel}}{s} \approx \frac{r}{s} \sqrt{\frac{2E_k}{m}}, \quad (4)$$

where  $m$  is the particle mass. Two problems arise from this simple formula: First, the velocities  $v_{\parallel}$  and  $v_{\perp}$  are not constant in the trap, as the particles are slowed down and focused (or defocused, see Ref. [18]) inside the mirrors. Second, the exact distance  $s$  between the neutralization point in the trap and the MCP is unknown. The importance of these two effects, which can smear the radial distribution measurement, will be treated separately using numerical simulation, as described in the next Section.

### 3 Numerical simulations

In order to verify the different approximations made in the derivation of Eq. 4, and to provide a better understanding of the trap behavior, we have performed numerical simulations of the particle trajectories in the actual potentials of the ion trap. The calculations were carried out using SIMION [20], which can solve the Laplace equation for a specific potential configuration in space and propagate ions on the computed potential grid. The program uses a fourth-order Runge-Kutta method to solve the Newtonian equations of motion. The density of ions in the trap is assumed to be low enough for ion-ion interactions to be neglected, and the trajectories are calculated for one ion at a time (the actual number of ions in the trap was of the order of  $10^5$  ions per injection).

For different values of  $V_z$ , while keeping the other potentials constant, we have traced the stable trajectories, starting from an initial distribution that covers the whole transverse stable (i.e., trapped) phase space of the electrostatic trap, as described in Ref. [18]. The stable phase space was found by systematically

varying the initial conditions of the particles. A stable trajectory was defined as one for which a propagated ion was trapped for more than 500  $\mu\text{s}$  (about 200 oscillations for 4.2 keV  $\text{Ar}^+$ , or 90 for 4.2 keV  $\text{Au}^+$ ). It was found that ions in unstable trajectories were usually lost from the trap after a few oscillations ( $< 20 \mu\text{s}$ ). The calculations were made using a constant integration time step, and the positions and velocities of the ions were recorded in a file at each of these time steps. Using this information, simulated distributions for the radial distribution at the MCP were calculated by assuming an equal probability for neutralization at each of these integration time steps, and propagating the (neutral) particles in straight lines, using the initial positions and velocities as recorded. This method has the advantage of representing faithfully the local ion density along the length of the trap. Implicit in the assumption of equal probability of neutralization in each time step is the assumption that the neutralization cross section is independent of kinetic energy for energies below 4.2 keV[21], even in the mirrors where the kinetic energies approach zero. The results can then be directly compared to the experimental distributions.

#### 4 Experimental and Simulation Results

Figure 2 shows a comparison between the measured (dotted line) and simulated (solid line) normalized distributions for the distance squared ( $P(r^2)$ ) at the MCP for 4.2 keV  $\text{Au}^+$ , and  $V_z=3200 \text{ V}$ . We choose to plot the  $r^2$  distributions as they display the radial density information in the most relevant manner. The number of particles located in an interval of width  $d(r^2) = 2rdr$  is proportional to the number of particles in the ring between  $r$  and  $r + dr$ , whose area is given by  $2\pi r dr$ . Similar distributions were measured for  $\text{Ar}^+$  and angiotensin  $\text{II}^+$  ions. Each of the measured distributions was characterized by the standard deviation of the radial distribution which in the present case is equal to the square root of the mean of  $r^2$ :  $\sigma_r = \sqrt{\langle r^2 \rangle}$ . Using Eq. 4, and replacing  $r$  by  $\sigma_r$  and  $s$  by the distance from the center of the trap to the MCP, typical transverse velocities  $v_\perp$  could be obtained for the different masses and values of the Einzel lens voltage ( $V_z$ ). Figure 3 shows the results for the three different ions as a function of  $V_z$ . Only a weak dependence of transverse velocity  $v_\perp$  on  $V_z$  is observed, except for  $\text{Ar}^+$  around 3250 V. The ratio  $v_\perp/v_\parallel \approx 9 \times 10^{-3}$  is found to be approximately constant for all ions.

Based on the excellent agreement between the experimental data and the simulations (see Fig. 2), one can now use the simulation to check the assumptions which led to Eq. 4, especially the assumption related to the contribution of the neutral particles produced inside the mirrors to  $P(r^2)$  and the unknown distance between the neutralization point and the MCP. Figure 4 shows an example of the distribution of the square of the transverse velocity  $P(v_\perp^2)$  from Simion simulations. The case presented is for all stable  $\text{Ar}^+$  ions in the field-

free region of the trap, for an Einzel lens voltage of  $V_z=3300$  V. To compare this distribution to the experimentally deduced typical transverse velocity, we characterize this distribution in a similar way as the squared radial distribution (see Fig. 2), using the square root of its mean, which is equivalent to the standard deviation of the TVD, yielding  $\sigma_{v\perp}=1.16$  mm/ $\mu$ s. This value is slightly lower than the one derived directly from the measured radial distributions (see Fig. 3), as can be expected since the latter includes some contributions from slower ions inside the mirrors that tend to have also larger  $v_{\perp}/v_{\parallel}$  ratio. However, the difference is relatively small (the reduced detection efficiency of the MCP for the slower particles also contributes to the fact that these have a minor effect on the measured distributions), and we conclude that the data shown in Fig. 3 are an upper limit of the transverse velocity of the trapped ions in the central (field-free) region of the trap.

## 5 Transverse phase space

The results obtained in the previous section show that the measured and simulated transverse velocities are in good agreement. Since the simulated value is obtained by filling the stable phase space of the trap, one can conclude that the ions stored in the trap always fill the available (stable) transverse phase space. This has an important implication as far as the ion loss processes are concerned. As pointed out previously [18], two processes play an important role in limiting the lifetime of the ions in the trap. The first is neutralization of the ions via charge exchange with the residual gas molecules, and the second is multiple scattering, which increases the transverse velocity of the ions until they reach the limit of the stable transverse phase space. Although the importance of the neutralization process can be observed experimentally by counting the number of neutral particles exiting the trap, the importance of multiple scattering is more difficult to observe experimentally. Also, it is quite clear that the loss due to neutralization is independent of the trap configuration, while the loss due to multiple scattering will be strongly dependent on the available transverse phase space, if the stable transverse phase space is always full. The fact that the measured transverse velocity is found to be equal to the one extracted from a simulated "full transverse phase space" suggests that the loss due to multiple scattering is very important, and that the lifetime of the ions is mostly limited by this process, a conclusion which was already reached by Pedersen et al. [18] using arguments based on known angular scattering cross sections.

In order to demonstrate the importance of multiple scattering as a loss process, we have calculated the area of the stable transverse phase space for the  $\text{Ar}^+$  ions as a function of the Einzel lens voltage  $V_z$ . The area was calculated by recording the transverse position and velocity for each pass of a stable ion



through the midplane of the trap. A scatter plot of these coordinates was then made, and the area filled by the points was estimated by dividing the phase space into a fine grid and counting the number of cells for which at least four points were found. These cells are then called "stable cells" (the minimum number of points required for a cell to be defined as stable has only a small influence on the final results). Fig. 5(a) shows the results of such a calculation as a function of  $V_z$ , while Fig. 5(b) shows the lifetime of the ions in the trap, as obtained by measuring the rate of neutral Ar hitting the MCP as a function of storage time and fitting the decay using an exponential function. A clear correspondence between the lifetime and the area of the transverse phase space is observed, including the dip around  $V_z=3200$  V.

## 6 Conclusions

We have measured the transverse velocity distribution of 4.2 keV  $\text{Ar}^+$ ,  $\text{Au}^+$ , and argon  $\text{II}^+$  stored in a linear electrostatic ion trap. The results show that the width of the TVD is mass dependent, and represents about 1% of the longitudinal beam velocity for the present trap geometry. The experimental results are in excellent agreement with the numerical simulation. More important, it shows that in the existing experimental setup, the phase space of the trap is filled very soon after injection. Thus, we can expect multiple scattering to be an important ion loss process (the other being neutralization). This is also demonstrated by the correlation between the area of transverse phase space and the measured lifetimes.

A consequence of our results is that the lifetime in the trap will also be a function of the trap length. Indeed, for a given angular dispersion of the beam and for a given mirror geometry, a trap with longer distance between the mirrors will be less stable, as the particles will be further away from the central axis of the trap when they enter the mirrors. On the other hand, although shorter traps will probably be more stable, they can store less ions.

The tool that we have developed to measure the transverse velocity distribution of the stored ions can now be used in studies of transverse cooling. Specifically, if a kicker for stochastic cooling is installed in the field-free region of the trap, it should be possible to shrink the  $r^2$  distribution, and thereby increase the storage lifetime. Moreover, because of Coulomb repulsion between the ions (especially near the turning points in the mirrors) and the radial mixing induced by the mirror, we can expect that transverse cooling will also affect the longitudinal velocity distribution.

This work was supported in part by the Israel Science Foundation. Laboratoire Kastler Brossel is Unité Mixte de Recherche du CNRS no. 8552, of the

## References

- [1] W.Paul and H.Steinwedel, Z. Naturforsch A **8** 448 (1953).
- [2] For a review on ion trapping, see Phys. Scripta. **T59** (1995), and *proceedings of the Conference on Trapped Charged Particles and Fundamental Interactions*, J. Phys. B **36**, issue 3 and 5 (2002).
- [3] D. Zajfman et al., Phys. Rev. A **55**, 1577 (1997).
- [4] M. Dahan et al., Rev. Sci. Instrum. **69**, 76 (1998).
- [5] R. Wester, K.G. Bhushan, N. Alstein, D. Zajfman, O. Heber, and M.L. Rappaport, J. Chem. Phys. **110**, 11 830 (1999).
- [6] K.G. Bushan, H.B. Pedersen, N. Alstein, O. Heber, M.L. Rappaport, and D. Zajfman, Phys. Rev. A **62**, 012504 (2000).
- [7] A. Wolf, K.G. Bhushan, I. Ben-Itzhak, N. Alstein, D. Zajfman, O. Heber and M.L. Rappaport, Phys. Rev. A **59**, 267 (1999).
- [8] L. Knoll, K.G. Bhushan, N. Alstein, D. Zajfman, O. Heber and M.L. Rappaport Phys. Rev. A **60**, 1710 (1999).
- [9] A. Diner et al., Phys. Rev. Lett. **93**, 063402 (2004).
- [10] A. Naaman et al., J. Chem. Phys., 113 4662 (2000)
- [11] H.B. Pedersen, D. Strasser, S. Ring, O. Heber, M.L. Rappaport, Y. Rudich, I. Sagi and D. Zajfman, Phys. Rev. Lett. **87** 055001-1 (2001).
- [12] S. Goldberg, D. Strasser, O. Heber, M. L. Rappaport, A. Diner, and D. Zajfman, Phys. Rev. A **68**, 043410 (2003).
- [13] S. P. Møller, Nucl. Instrum. Methods in Physics Research A **394**, 281 (1997).
- [14] S. P. Møller and U. V. Pedersen, Phys. Scripta **T92**, 105 (2001).
- [15] U. V. Pedersen, M. Hyde, S. P. Møller and T. Andersen, Phys. Rev. A **64**, 012503-1 (2001)
- [16] K. Hansen, J. U. Andersen, P. Hvelplund, S. P. Møller, U. V. Pedersen, and V. V. Petrunin, Phys. Rev. Lett. **87**, 123401 (2001).
- [17] F. Hillenkamp et al., Anal. Chem **63**, 1193A (1991)
- [18] H.B. Pedersen, D. Strasser, O. Heber, M.L. Rappaport and D. Zajfman, Phys. Rev. A **65** 042703 (2002).

- [19] L. K. Johnson, R. S. Gao, C. L. Hakes, K. A. Smith, and R. F. Stebbings, Phys. Rev. A **40**, 4920 (1989).
- [20] SIMION, Version 6.0, Ion Source Software (<http://www.srv.net/~klack/simion.html>).
- [21] G. J. Lockwood, Phys. Rev. A **2**, 1406 (1970).

## Figures

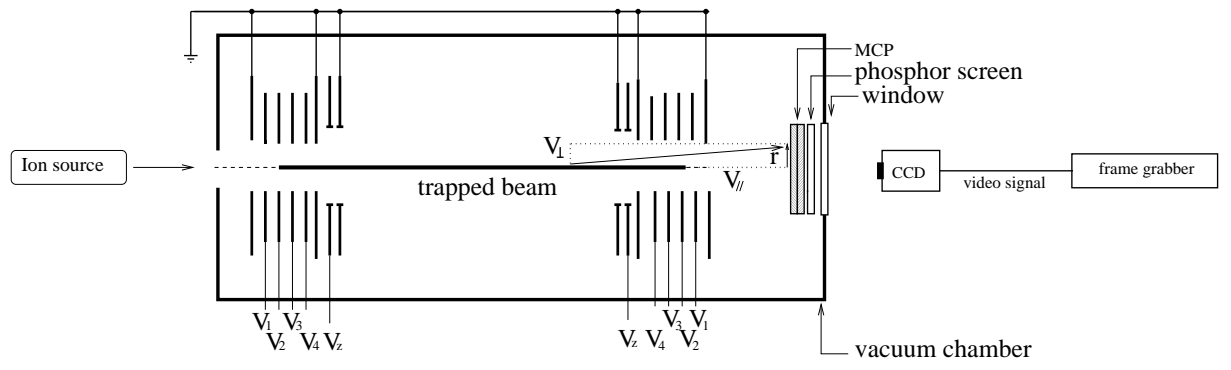


Fig. 1.

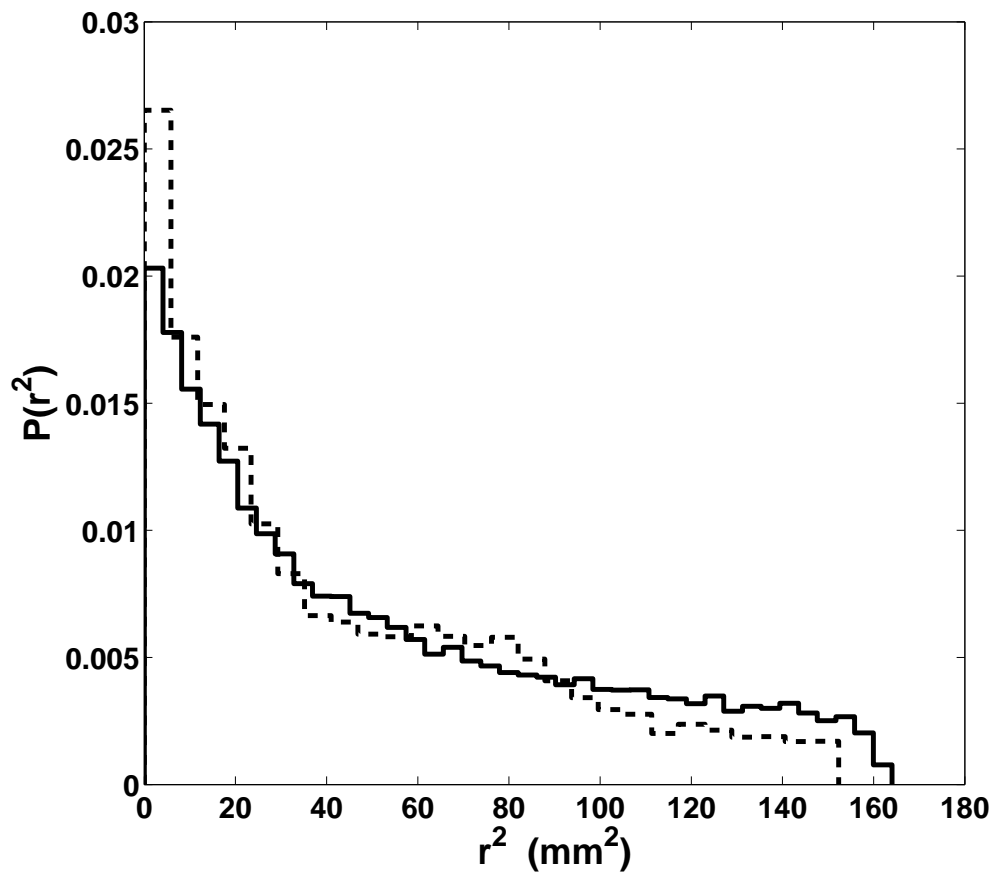


Fig. 2.

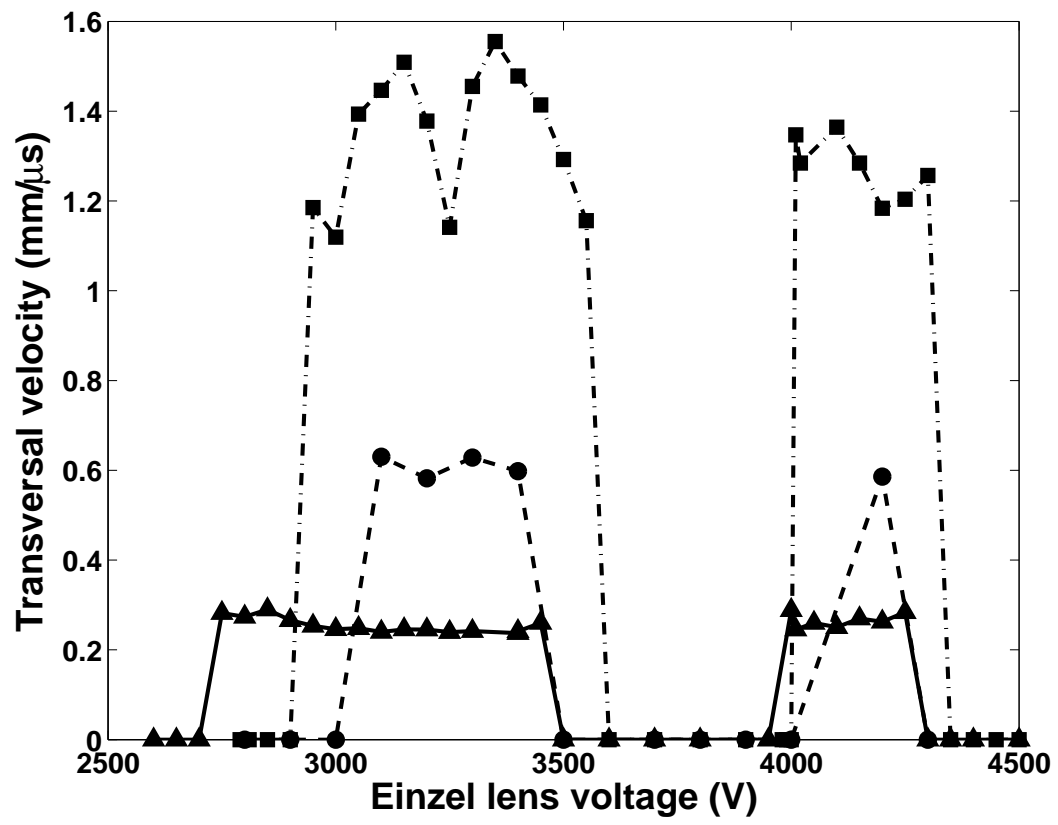


Fig. 3.

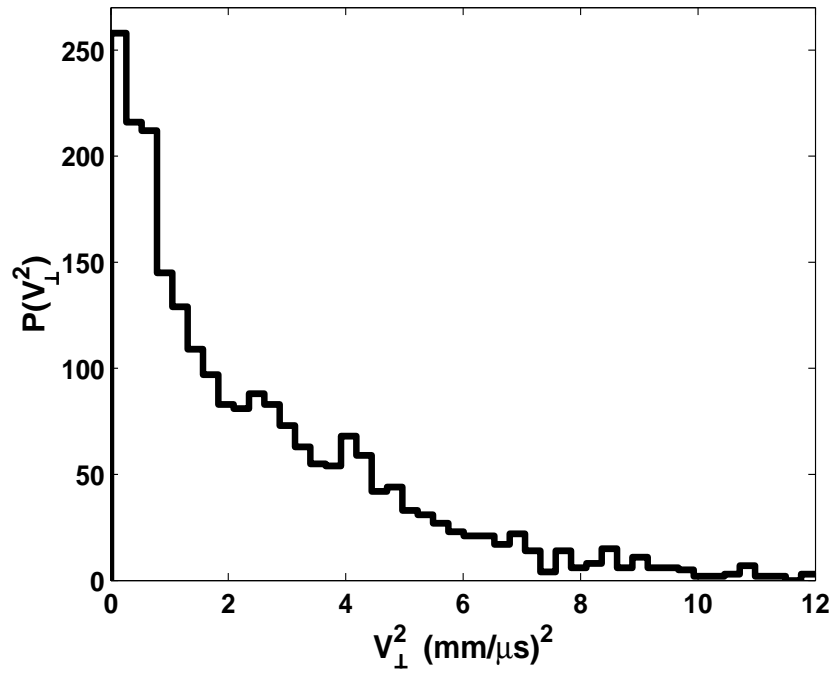


Fig. 4.

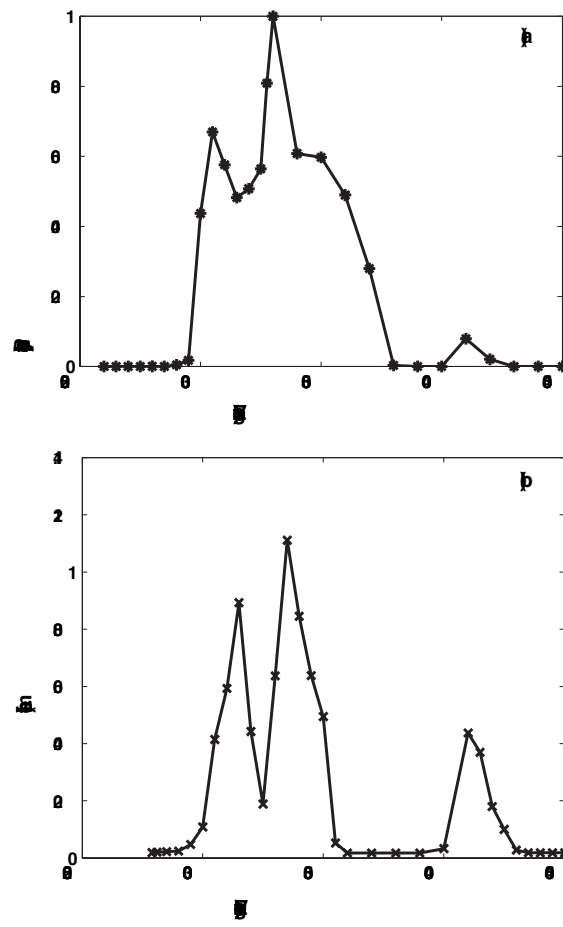


Fig. 5.



## Figure Captions

- Fig. 1: Schematic view of the experimental setup. The bunch is injected through the left hand side of the trap (entrance electrodes), and the neutral particles escaping from the trap through the exit electrodes are counted by the MCP detector, whose phosphor screen is imaged by a CCD camera. The drawing is not to scale.
- Fig. 2: Normalized  $r^2$  distributions for 4.2 keV  $\text{Au}^+$ . Dotted line: measured by the MCP detector; solid line: simulation with Simion[20]. The Einzel lens voltage was 3200 V.
- Fig. 3: Measured transverse velocity as a function of the Einzel lens voltage for three different ions:  $\text{Ar}^+$  (■);  $\text{Au}^+$  (●); angiotensin  $\text{II}^+$  (▲). The transverse velocity is set to zero for unstable configurations.
- Fig. 4: Calculated transverse velocity distribution in the field-free region of the trap for  $\text{Ar}^+$  ions with  $V_z=3300$  V.
- Fig. 5: (a) Area of the stable transverse phase space in the midplane of the trap as a function of  $V_z$ . (b) Measured lifetime for  $\text{Ar}^+$  as a function of  $V_z$ .